PHYSICAL REVIEW A VOLUME 55, NUMBER 3 MARCH 1997

Manifestations of atomic and core resonances in photoelectron energy spectra

Lars G. Hanson,[1] Jian Zhang,[1] and P. Lambropoulos[1,2]
[1]*Max-Planck-Institut für Quantenoptik, Hans-Kopfermann-Strasse 1, D-85748 Garching, Germany*
[2]*Foundation for Research and Technology Hellas, Institute of Electronic Structure and Laser, P.O. Box 1527, Heraklion 71110, Crete, Greece*

(Received 30 August 1996)

The manifestation of atomic and core resonances in photoelectron energy spectra of two-electron atoms is discussed in detail. An approach to the general problem of elimination of strongly coupled continua is presented and quantitative requirements for the validity of the theory are obtained. The theory is applied to calcium thus providing a theoretical interpretation of, and additional insight into, all features of an experiment by Walker *et al.* [Phys. Rev. Lett. **75**, 633 (1995)]. [S1050-2947(97)07203-X]

PACS number(s): 32.80.Rm, 32.80.Fb, 32.80.Wr

The excitation of two electrons above the first ionization threshold leads to manifolds of doubly excited states whose dominant mode of decay is autoionization, with one electron ejected and the ion left either in its ground or in one of its excited states, depending on the level (energy) of excitation. The process of autoionization is a manifestation of electron-electron interaction and correlation, as is the process of two-electron excitation, especially when accomplished via single photon absorption. The end result, under weak excitation in lowest nonvanishing order of perturbation theory, is irreversible decay into the ionization continuum. This is the context of studies of traditional autoionization [2–5] over the last three decades.

The situation changes considerably under multiphoton and/or coherent excitation by stronger electromagnetic fields. In the simplest generalization, even single-photon excitation of an autoionizing state (AIS) by a relatively strong field — such that the strength of excitation is comparable to or larger than the strength of autoionization — the coupling to the continuum may not be necessarily irreversible and in fact part of the population may be trapped in a coherent superposition of the ground and the AIS. This trapping and stabilization of AIS was first predicted [6] fifteen years ago but it is only recently that it was observed experimentally [7], while its relevance to amplification without inversion and related nonlinear optics has also attracted theoretical interest [8]. Excitation through few photon processes, in addition to the obvious advantage of accessing manifolds of higher angular momenta, also offers the possibility of selective excitation through the combination of more than one wavelength. The latter has formed the basis of the so-called isolated core excitation technique, introduced and exploited extensively by Gallagher and collaborators [9], and continues to provide a versatile tool for the study of highly excited autoionization manifolds [10]. The combination of few-photon excitation — involving one or more wavelengths — with stronger fields can also be exploited to generate novel effects, some of which are the subject of this paper.

A most fundamental scheme of double electron excitation in two electron atoms, such as the alkaline earth atoms, is to raise one electron to a Rydberg state and either at the same time or sequentially raise the other electron to the first excited ionic state. With the ground state configuration of the valence shell of alkaline earth atoms being of the form $(ns)^2\,{}^1S_0$, the resulting doubly excited configurations are then of the form $(n'lnp)^1P_1$. If a single Rydberg state $n'l$ is excited via a single or few photon absorption, we have a typical case of an isolated core excitation scheme [9]. If, in addition, the transition ns-np was driven strongly, we would have ac Stark splitting and stabilization phenomena of the type discussed in Refs. [6–8]. If, on the other hand, instead of exciting a single Rydberg state $n'l'$, we were to excite a group of them through an appropriately short, coherent pulse, a radial Rydberg wave packet would be created. Now, the strong driving of the core transition ns-np, with a Rabi period which may be of the magnitude of the Kepler period of the wave packet, can be expected to lead to novel effects on the evolution of the wave packet as the timing can be such that, upon returning to the core, the wave packet may find the other electron (i.e., the core) either in the ground or the excited state [11–13]. An excited core would tend to cause decay of the wave packet (through autoionization) while a ground state core would simply lead to the usual dispersion. Much, however, will depend on the relative magnitudes of three important characteristic times, namely, the Kepler period, Rabi period of the core transition, and autoionization lifetime. It is moreover possible to create entangled wave packet and core states [11].

A further generalization of the above situation can be contemplated if instead of a superposition of bound Rydberg states $n'l$ we have a transition into the continuum (i.e., a wave packet of positive energy states), while at the same time the photon frequency is such as to match the core transition. Now both steps occur simultaneously, because otherwise the electron in the continuum will depart before an interaction reflecting the excitation of the core can be manifested. This scenario can therefore be most easily realized under excitation and ionization by one radiation source whose frequency exactly matches the ionic core ns-np transition. Again a strongly driven core transition would lead to ac Stark splitting whose manifestation would have to be sought in the photoelectron energy spectrum (PES), since a wave packet of positive energy states does not return to the core once the pulse is over. We discuss below in more detail the expected features of this effect, but for the moment the point to be kept in mind is the connection with the previous effect on the wave packet, namely the manifestation on an electromagnetically driven core transition on a second electron, mediated by electron-electron interaction.

Although experimental implementations as well as the theoretical discussion of the two phenomena differ in detail, their formal and conceptual aspects are very similar to the point of being parts of the same general formal structure. The bulk of this paper deals with the second problem, namely, the effect of a strongly driven core transition on the PES. We shall, however, begin the formal development in all its generality encompassing both phenomena.

The strong driving of a resonant transition between two discrete states causes, as noted above, an ac Stark splitting, usually detected through another transition involving the same electron. Walker *et al.* [1] have observed in Ca the effect of ac Stark splitting of an ionic core transition on the photoelectron energy spectrum (PES) of the atom. Their motivation came from theoretical predictions by Grobe and Eberly [14] based on a one-dimensional model of a negative ion. The nature of the splitting is always the same, but the process through which it is probed may vary. It can be resonance fluorescence [15] from the upper to the lower level, probe absorption [16] from the upper level to a (higher) third one (double optical resonance), or the PES [17] if the driving field is sufficiently strong to cause ionization. In fluorescence and photoionization, no additional probe is necessary since the energy splitting is manifested in the energy analysis of a transition from the upper state of the two-level system into a continuum; the photon continuum in fluorescence, the atomic continuum in ionization.

The new twist of interest here is that one electron undergoes Rabi oscillations, while a second is ionized carrying along the information on the splitting, because the electrons interact. Thus, although the splitting results from the strong coupling between two discrete states of the ion, from the standpoint of the two-electron system it represents coupling between two states in the continuum (above the ionization threshold); hence the term continuum-continuum Autler-Townes splitting employed in [1]. We must, however, emphasize that the coupling of these continua of the two-electron system is not smooth, as they have the core discrete-discrete transition embedded in them. Stark splitting in the transition between two smooth continua (such as those of the hydrogen atom) is not possible.

The model was extended by Grobe and Haan [18] to account formally for a possible extra near-resonant atomic (autoionizing) state. The subtle interplay involving the ionic transition and the inevitably present *corresponding* atomic transition, differing only by the spectator electron, was not included. In order for the theory to be applicable to the interpretation of an experiment, however, the atomic transition as well as other atomic or ionic states, depending on the atom, need to be included as we have shown in a short communication elsewhere [19].

The purpose of this paper is to present first the necessary formal framework for a qualitative understanding and interpretation of relevant experiments taking into account the above interwined effects. Given the existence of experimental results on Ca, we have chosen to address this specific problem quantitatively and to compare our predictions with the data. This understanding requires the reliable calculation of the necessary atomic parameters, which is a project in itself. It has been accomplished through techniques and computer programs that we have developed in a broader context over the last few years. The detailed comparison of theoretical results with the experimental data has enabled us to sort out the significant effects that lead to somewhat unexpected features.

The formal treatment of this type of problem, in a realistic context, is rather intricate as it involves a number of interwined effects. The successive approximations leading to the sets of parameters and equations necessary for the interpretation of experiments within the appropriate range of laser intensities require careful examination and justification. In order to facilitate the reading of the paper, we have chosen to relegate to Appendixes significant parts of the formal development, keeping in the main body of the paper the basic theoretical structure that is necessary for at least a qualitative comprehension of the underlying physics.

I. FORMULATION

We adopt in the general formulation of the problem the quantized form of the radiation field which, although not necessary, makes the initial discussion more transparent. To be specific, and in view of the detailed calculations in Ca that we present later on, we consider the initial atomic state as $(4s)^2\,{}^1S_0$ in the presence of a monochromatic radiation source of frequency ω and N photons in the initial state. The excited atomic state $4s4p\,{}^1S_0$ will also be of importance in some problems, but it must be distinguished from the ionic first excited $\mathrm{Ca}^+(4p)$. We shall be interested in the case for which $\hbar\omega$ is near resonance with the transition $\mathrm{Ca}^+(4s\text{-}4p)$, which here means tunable around 25 340 cm^{-1}. The atomic energy difference $\mathrm{Ca}(4s4p)$-$\mathrm{Ca}(4s)^2$ is 23 652 cm^{-1}, which although displaced by almost 2000 cm^{-1} from the ionic resonance is nevertheless sufficiently close to require special attention above certain intensities, as we show in the following sections. This is not a feature of Ca only but is to be expected to varying degree in all alkaline earth atoms. We define then two relevant system (atom plus field) states as $|g\rangle=|\,\mathrm{Ca}(4s)^2\,{}^1S_0;N\rangle$ and $|\overline{g}\rangle=|\,\mathrm{Ca}(4s4p)^1\,P_1;N-1\rangle$. Two of the photons in this frequency range are energetically sufficient to ionize the atom whose ionization threshold is at 49 305 cm^{-1}. Thus system states of the form $|c\rangle=|\,\mathrm{Ca}^+4s+e^-_{\epsilon_c};N-2\rangle$, where $|c\rangle$ implies atomic continuum of positive energy ϵ_c, are also to be included. Due to the near resonance of the photon frequency with the $4s$-$4p$ ionic core transition, once one electron is lifted into the continuum — or even to high Rydberg states—the state $\mathrm{Ca}^+(4p)$ becomes strongly coupled via the absorption of one more photon, bringing thus into play the states $|\overline{c}\rangle=|\,\mathrm{Ca}^+4p+e^-_{\epsilon_c};N-3\rangle$ involving the same atomic continuum as in $|c\rangle$ but an excited core state. The respective energies of the states defined above are $E_g=E(\,\mathrm{Ca}(4s)^2\,{}^1\,S_0)+N\hbar\omega$, $E_{\overline{g}}=E(\mathrm{Ca}(4s4p)^1\,P_1)+(\mathrm{N}-1)\hbar\omega$, $E_c=E(\mathrm{Ca}^+4s)+\epsilon_c+(N-2)\hbar\omega$, and $E_{\overline{c}}=E(\,\mathrm{Ca}^+4p)+\epsilon_c+(N-3)\hbar\omega$. Although $|\overline{c}\rangle$ differs from $|c\rangle$ by the excitation of the core electron with the continuum state being the same, still technically speaking $|\overline{c}\rangle$ is another continuum (of higher energy) as far as the two-electron system is concerned. These two continua are coupled by a dipole transition which, however, is significantly different from the transition between two continuum states in above threshold ionization (ATI) in a one-electron atom or model of an atom.

Leaving other states out for the moment, we have a subspace in which we can formulate the essential features of the problem. If we introduce the projection operators $P=|g\rangle\langle g|$, $Q_{\bar{g}}=|\bar{g}\rangle\langle\bar{g}|$, $Q_j=\int dc_j|c_j\rangle\langle c_j|$, and $\bar{Q}_j=\int dc_j|\bar{c}_j\rangle\langle\bar{c}_j|$, where we have added an index j in the continua to account for the possibility of the involvement of further continua, as will indeed be the case, the identity operator can be written as

$$\mathbb{1}=P+Q_{\bar{g}}+\sum_j Q_j+\sum_j \bar{Q}_j . \tag{1}$$

The Hamiltonian is as usual of the form

$$H=H^A+H^R+D\equiv H^0+D, \tag{2}$$

where H^A and H^R are the free atom and free field Hamiltonians, respectively, with D being the interaction between the two, in the dipole approximation.

A. Square pulse

To establish the formal equations governing the dynamics, we assume for the moment (but relax later on) a constant field amplitude (square pulse) so that we can make use of the resolvent operator $G(z)\equiv(z-H)^{-1}$, with z being a complex number, the variable of the Laplace transform of the time evolution operator from which $G(z)$ has resulted [20].

The projection operators introduced above enable us to partition the Hamiltonian in a convenient way. Thus the projected Hamiltonian operators PHP, $Q_{\bar{g}}HQ_{\bar{g}}$, Q_jHQ_j, and $\bar{Q}_jH\bar{Q}_j$ have as eigenstates the respective sets of states introduced earlier, while the couplings between these sets of states enter through matrix elements of nondiagonal operators such as PHQ_j, $PHQ_{\bar{g}}$, and $Q_jH\bar{Q}_j$. The couplings entering the first will be treated perturbatively to the appropriate order, while the coupling through the second and third needs to be treated exactly between the states of concern.

The procedure through which one obtains the coupled equations of the relevant matrix elements of G, namely, G_{gg}, $G_{\bar{g}g}$, G_{cg}, and $G_{\bar{c}g}$ is well established [20] and need not be reproduced here. The couplings between the various subspaces are $D_{g\bar{g}}$, which is the dipole operator between two atomic states, the two-photon coupling $D^{(2)}_{cg}$, which represents an effective two-photon (ionization) dipole matrix element [21] given by

$$D^{(2)}_{cg}=\sum_n \frac{D_{cn}D_{ng}}{E_n-E_g} \tag{3}$$

with $|n\rangle$ being system states of the form $|\mathrm{Ca}(4snp)\,{}^1P_1;N-1\rangle$ where $n>4$, including the respective continuum, and similar self-explanatory couplings such as $D_{\bar{g}c}$, $D^{(2)}_{g\bar{c}}$, and finally the coupling between $|c\rangle$ and $|\bar{c}\rangle$ entering through the matrix elements of $Q_jH\bar{Q}_j$, which in the simplest approximation would be reduced to $D_{c\bar{c}}$, a point to be discussed later on.

The equations for the pertinent matrix elements of G in the most general form are

$$(z-E_g)G_{gg}-D_{g\bar{g}}G_{\bar{g}g}-\sum_j\int dc_j\langle g|PHQ_j|c_j\rangle G_{c_jg}=1, \tag{4a}$$

$$-D_{\bar{g}g}G_{gg}+(z-E_{\bar{g}})G_{\bar{g}g}-\sum_j\int dc_j[\langle\bar{g}|Q_{\bar{g}}H\bar{Q}_j|\bar{c}_j\rangle G_{\bar{c}_jg}+\langle\bar{g}|Q_{\bar{g}}HQ_j|c_j\rangle G_{c_jg}]=0, \tag{4b}$$

$$-\langle c_j|Q_jHP|g\rangle G_{gg}-\langle c_j|Q_jHQ_{\bar{g}}|\bar{g}\rangle G_{\bar{g}g}+(z-E_{c_j})G_{c_jg}-\sum_j\int dc'_j\langle c_j|Q_jH\bar{Q}_j|\bar{c}'_j\rangle G_{\bar{c}'_jg}=0, \tag{4c}$$

$$-\langle\bar{c}_j|\bar{Q}_jHQ_{\bar{g}}|\bar{g}\rangle G_{\bar{g}g}-\sum_j\int dc'_j\langle\bar{c}_j|\bar{Q}_jHQ_j|c'_j\rangle G_{c'_jg}+(z-E_{\bar{c}_j})G_{\bar{c}_jg}=0. \tag{4d}$$

First, observe that, since as noted earlier the coupling between the continua $|c\rangle$ and $|\bar{c}\rangle$ reduces to the coupling between the $4s$ and $4p$ ionic states, there is no change in the angular momentum (partial wave) of the continuum wave function. That is why only terms with the same j occur in matrix elements coupling $|c\rangle$ with $|\bar{c}\rangle$. Using the definition of the projection operators, it is straightforward to see that

$$\langle g|PHQ_j|c_j\rangle=D^{(2)}_{gc_j}\ \text{and}\ \langle\bar{g}|Q_{\bar{g}}H\bar{Q}_j|\bar{c}_j\rangle=D^{(2)}_{\bar{g}\bar{c}_j},$$

which represent relatively weak two-photon transitions in the sense that they raise the electron into the continuum irreversibly, without an oscillation back to the bound state by the same transition amplitude. This means that they can be treated perturbatively in dealing with the set of Eqs. (4a)–(4d). Since the initial state is $(4s)^2$, two-photon ionization leads to two continua (partial waves) s and d, indexed by j in the equations above. These two continua draw electrons from the ground state independently, and, as noted earlier, the coupling matrix elements do not mix the j's. Thus the two vertical parts of Fig. 1 can be thought of as separate, up to a certain intensity beyond which higher order contributions begin entering. We can therefore consider first the dominant continuum, namely d, and develop the formal treatment for that case. At the end, whenever we show results, we have always included the effect of continuum s, which is simply additive to the overall process. It also happens in this case, to give much smaller contribution than the d continuum.

We consider then the right-hand vertical half of Fig. 1, which means that we drop the index j and the summation in Eqs. (4a)–(4d), where $|c\rangle$ denotes the d continuum. Taking also into account the simplifications in the coupling matrix elements indicated above, the equations become

$$(z-E_g)G_g-D_{g\bar{g}}G_{\bar{g}}-\int dc D^{(2)}_{gc}G_c=1, \tag{5a}$$

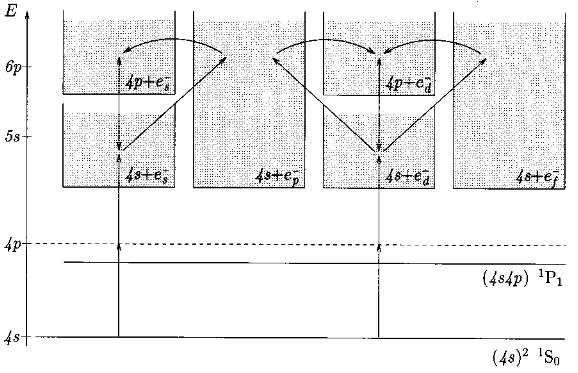

FIG. 1. Level scheme for Ca$^+$ (on axis) and Ca. Curved arrows signify configuration interaction, while straight arrows are field couplings.

$$-D_{\bar g g}G_g+(z-E_{\bar g})G_{\bar g}-\int dc[D_{\bar g c}G_c+D^{(2)}_{\bar g\bar c}G_{\bar c}]=0, \tag{5b}$$

$$-D^{(2)}_{cg}G_g-D_{c\bar g}G_{\bar g}+(z-E_c)G_c-\int dc'\langle c|Q_cH\bar Q_c|\bar c'\rangle G_{\bar c'}=0, \tag{5c}$$

$$-D^{(2)}_{\bar c\bar g}G_{\bar g}-\int dc'\langle \bar c|\bar Q_cHQ_c|c'\rangle G_{c'}+(z-E_{\bar c})G_{\bar c}=0, \tag{5d}$$

where in order to compress notation we have omitted the common right-hand index g in the matrix elements of G, and to avoid confusion, we have renamed the projection operators Q_j and $\bar Q_j$ as Q_c and $\bar Q_c$, since we now have one continuum c.

The most subtle part of these equations now is in the matrix elements $\langle c|Q_cH\bar Q_c|\bar c'\rangle$ involving coupling of two continua and integration over one of them. These are continua of the two-electron system with one electron in a bound state and the other in a continuum state. Qualitatively, it represents a matrix element of the type $\langle \mathrm{Ca}^+(4s)|r|\mathrm{Ca}^+(4p)\rangle\langle\epsilon|\epsilon'\rangle$ where the two continuum states represent the same partial wave seeing different cores $4s$ and $4p$. It is often the case that couplings of continua of this type can be separated into two parts: one having a smooth dependence on the energies ϵ and ϵ', and the other a delta function $\delta(\epsilon-\epsilon')$, also referred to as off- and on-the-energy shell contributions. Depending on the problem, the δ-function part may be the dominant one, in which case the simplification in the set of Eqs. (5a)–(5d) is evident, since the integrals coupling the two continua are trivially performed leaving only the integrals in Eqs. (5a) and (5b) coupling the continua with discrete states.

It does indeed turn out that this is the case here and that to a very good approximation it is only the resonant (on-the-energy shell) part that is significant. The arguments justifying these statements are outlined in Appendix A. The net result, which allows us to continue with a more tractable set of equations, is that we can take $\int dc'\langle \bar c|\bar Q_cHQ_c|c'\rangle G_{c'}=D_{\bar c c}G_c$ and similarly $\int dc'\langle c|Q_cH\bar Q_c|\bar c'\rangle G_{\bar c'}=D_{c\bar c}G_{\bar c}$, which then substituted into Eqs. (5a)–(5d) reduce them to the form

$$(z-E_g)G_g-D_{g\bar g}G_{\bar g}-\int dcD^{(2)}_{gc}G_c=1, \tag{6a}$$

$$-D_{\bar g g}G_g+(z-E_{\bar g})G_{\bar g}-\int dc[D_{\bar g c}G_c+D^{(2)}_{\bar g\bar c}G_{\bar c}]=0, \tag{6b}$$

$$-D^{(2)}_{cg}G_g-D_{c\bar g}G_{\bar g}+(z-E_c)G_c-D_{c\bar c}G_{\bar c}=0, \tag{6c}$$

$$-D^{(2)}_{\bar c\bar g}G_{\bar g}-D_{\bar c c}G_c+(z-E_{\bar c})G_{\bar c}=0, \tag{6d}$$

where as shown in Appendix A the matrix elements $D_{c\bar c}$ are practically given by $\langle 4s|d|4p\rangle$ involving the ionic states only.

A few further comments on the on-the-energy shell approximation may be relevant here. The dipole coupling of the states $|c\rangle$ and $|\bar c\rangle$ is, from a formal point of view, a continuum-continuum coupling of the type that appears in above-threshold ionization (ATI). But it is different in a crucial way; the two coupled continua represent two-electron states with one of the electrons in a discrete state. We are therefore not dealing with smooth continua as is the case in a one-electron atom or in the so-called single active electron approximation in a more complex atom. What we have here are transitions between two-electron structured continua which allow the resonance approximation while the same approximation would not be justified in a typical ATI context of continuum-continuum transitions of a single electron.

Solving for G_c and $G_{\bar c}$ in Eqs. (5a)–(5d) yields

$$[z-E_g-I_{gg}(z)]G_g-[D_{g\bar g}+I_{g\bar g}(z)]G_{\bar g}=1, \tag{7a}$$

$$-[D_{\bar g g}+I_{\bar g g}(z)]G_g+[z-E_{\bar g}-I_{\bar g\bar g}(z)]G_{\bar g}=0, \tag{7b}$$

$$G_c=\frac{[(z-E_{\bar c})[D^{(2)}_{cg}G_g+D_{c\bar g}G_{\bar g}]+D_{c\bar c}D^{(2)}_{\bar c\bar g}G_{\bar g}]}{(z-E_c)(z-E_c+E_{\bar c})-|D_{c\bar c}|^2}, \tag{7c}$$

$$G_{\bar c}=\frac{[D_{\bar c c}(D^{(2)}_{cg}G_g+D_{c\bar g}G_{\bar g})+(z-E_c)D^{(2)}_{\bar c\bar g}G_{\bar g}]}{(z-E_c)(z-E_c+E_{\bar c})-|D_{c\bar c}|^2}. \tag{7d}$$

The shift-width integrals $I_{gg}(z)$, $I_{\bar g g}(z)$, $I_{g\bar g}(z)$, and $I_{\bar g\bar g}(z)$ are given in Appendix B and appear somewhat different from those normally encountered due to the strong coupling of continua. In that Appendix, we show that they nevertheless reduce to normal shifts and widths provided the continuum couplings can be considered *constant* over a range given by the Rabi frequency of the ionic transition. This requirement, which is more strict than the one required for doing the usual pole approximation, is satisfied below certain intensity (see Appendixes B and C), and leaves us with the following expressions:

$$I_{gg}\simeq\int dE_c\rho(E_c)\frac{|D^{(2)}_{cg}|^2}{E_g-E_c}\equiv s_g-\frac{i}{2}\gamma_g, \tag{8a}$$

$$I_{\bar g\bar g}\simeq\int dE_c\rho(E_c)\frac{|D_{c\bar g}|^2}{E_g-E_c}+\int dE_{\bar c}\bar\rho(E_{\bar c})\frac{|D^{(2)}_{\bar c\bar g}|^2}{E_g-E_{\bar c}}$$

$$\equiv s_{\bar g}-\frac{i}{2}\gamma_{\bar g}, \tag{8b}$$

$$I_{g\bar g}\simeq\int dE_c\rho(E_c)\frac{D^{(2)}_{gc}D_{c\bar g}}{E_g-E_c}\equiv s_{g\bar g}-\frac{i}{2}\gamma_{g\bar g}, \tag{8c}$$

$$I_{\bar g g}\simeq\int dE_c\rho(E_c)\frac{D_{\bar g c}D^{(2)}_{cg}}{E_g-E_c}\equiv s_{\bar g g}-\frac{i}{2}\gamma_{\bar g g}. \tag{8d}$$

In the integrals over states we have shown explicitly the densities of states ρ and $\bar\rho$, corresponding to the two continua. In the last step the pole approximation is implied leading to shifts s and ionization widths γ involving two-photon processes, as a result of which these shifts are not expected to be very important quantitatively. Shifts will be dominated by the first order contributions which we shall always incorporate in the energies, and which thus become intensity dependent. The matrix elements $\tilde D_{g\bar g}\equiv D_{g\bar g}+I_{g\bar g}$ and $\tilde D_{\bar g g}\equiv D_{\bar g g}+I_{\bar g g}$ are defined so as to include the non-Hermitian coupling through the continuum $|c\rangle$.

Using Eqs. (7c) and (7d) and the results from Appendix B we are now in a good position to estimate the significance of the error made by assuming the continuum-continuum coupling to be purely discrete, i.e., to estimate the validity of the on-the-energy shell approximation. This is done in Appendix C by evaluating the integrals involving the couplings ignored in assuming Eqs. (7c) and (7d) to be valid. The calculation reveals the limits of the range of parameters for which the theory applies, and for Ca is of the order of 10^{13} W/cm^2.

We return now to the problem of determining the PES. Let $z_g^{\pm}$ and $z_c^{\pm}$ be the roots of the second-order algebraic equations,

$$(z-z_g^+)(z-z_g^-)\equiv\left(z-E_g+\frac{i}{2}\gamma_g\right)\left(z-E_g+\Delta_g+\frac{i}{2}\gamma_{\bar g}\right)$$

$$-\tilde D_{g\bar g}\tilde D_{\bar g g}, \tag{9a}$$

$$(z-z_c^+)(z-z_c^-)\equiv(z-E_c)(z-E_c+\Delta_c)-|D_{c\bar c}|^2 \tag{9b}$$

with detunings defined by

$$\Delta_g\equiv E_g-E_{\bar g}=\hbar\omega-E(\mathrm{Ca}(4s4p)\,^1P_1)+E(\mathrm{Ca}(4s)^2\,^1S_0), \tag{10a}$$

$$\Delta_c\equiv E_c-E_{\bar c}=\hbar\omega-E(\mathrm{Ca}^+4p)+E(\mathrm{Ca}^+4s). \tag{10b}$$

For use in what follows, we also define the generalized Rabi frequencies of the atomic and ionic core transition by $\tilde\Omega_g=\sqrt{[\Delta_g-i/2\,(\gamma_g-\gamma_{\bar g})]^2+4\tilde D_{g\bar g}\tilde D_{\bar g g}}$ and $\tilde\Omega_c=\sqrt{\Delta_c^2+4|D_{c\bar c}|^2}$, respectively. Note that, although Δ_c does not depend on the continuum electron energy, but only on the detuning of $\hbar\omega$ from the ionic core transition, for convenience we retain the label c.

Introducing for brevity the quantity $Q(z)=(z-z_g^+)(z-z_g^-)(z-z_c^+)(z-z_c^-)$, we can write the solutions for G_c and $G_{\bar c}$ in the form

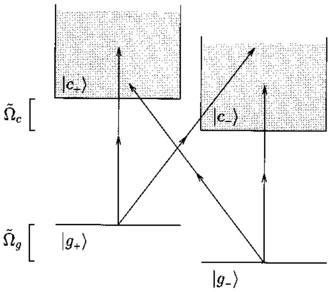

FIG. 2. The square-pulse spectrum is conveniently explained in a dressed-state basis. The field coupling of the bound states ($|g\rangle$ and $|\bar g\rangle$) and of the continua ($|c\rangle$ and $|\bar c\rangle$) are diagonalized independently providing dressed, uncoupled bound states ($|g_+\rangle$ and $|g_-\rangle$) and continua ($|c_+\rangle$ and $|c_-\rangle$). Due to the mixing each bound state is coupled to both continua and a four-peak spectrum is expected.

$$G_c=\left\{(z-E_{\bar c})\left[D^{(2)}_{cg}\left(z-E_{\bar g}+\frac{i}{2}\gamma_{\bar g}\right)+D_{c\bar g}\tilde D_{\bar g g}\right]\right.$$

$$\left.+D_{c\bar c}D^{(2)}_{\bar c g}\tilde D_{\bar g g}\right\}\Big/\,Q(z), \tag{11a}$$

$$G_{\bar c}=\left\{D_{\bar c c}\left[D^{(2)}_{cg}\left(z-E_{\bar g}+\frac{i}{2}\gamma_{\bar g}\right)+D_{c\bar g}\tilde D_{\bar g g}\right]\right.$$

$$\left.+(z-E_c)D^{(2)}_{\bar c g}\tilde D_{\bar g g}\right\}\Big/\,Q(z). \tag{11b}$$

From these expressions and the Laplace inversion integral, we obtain the time-dependent amplitudes $U_{cg}(t)$ and $U_{\bar c g}(t)$ for the transitions to the states $|c\rangle$ and $|\bar c\rangle$. We refrain from exhibiting these expressions, but only note that $|U_{cg}(t)|^2$ and $|U_{\bar c g}(t)|^2$ represent the probabilities of finding at time t a free electron and the core in either state $4s$ or $4p$, respectively. The readily measurable quantity, however, is the PES given by $S(t,\epsilon_c)=|U_{\bar c g}(t)|^2+|U_{cg}(t)|^2$, which in the long time limit (meaning complete ionization) can be shown to be time-independent, as also expected on physical grounds. In this case only the real poles $z_c^{\pm}$ of the resolvent give nonvanishing contributions to the time evolution of the amplitudes.

For a square pulse a four-peak spectrum is therefore expected in general, with the peak separations given by the Rabi frequencies of the core and atomic transitions. This is easily understood from a dressed state picture (Fig. 2) [20]. Each peak can be attributed to a transition from a dressed atomic state ($|g_+\rangle$, $|g_-\rangle$) to a dressed ionic continuum ($|c_+\rangle$, $|c_-\rangle$).

A final comment concerning the meaning and implications of Eqs. (6a)–(6d) may be useful before leaving this section. We have shown in Appendix A that the matrix element $D_{c\bar c}$ coupling the two continua reduces, under the conditions of this problem, to the matrix element $\langle 4p|r|4s\rangle$ between the two discrete states of the core. In fact the mathematical derivation in that Appendix involves a rather subtle procedure and almost counterintuitive result which is possible only because one of the electrons is in the continuum, as it is the integration over the principal value parts that leads to the cancellation reducing the expression to the core matrix element. Note that if the outer electron was not above the threshold but just below, in a high Rydberg state, the result would be different, in that it would involve an overlap integral between Rydberg wave functions seeing a ground and an excited core state. It is precisely that overlap that is reduced to unity through the principal value part integrals which would be absent in the case of Rydberg electrons. One might then be tempted to infer that electron-electron interaction and the concomitant correlation are not playing a role here. But that would be a misguided inference because correlation is already inherent in the fact that the energy of the core (ionic) resonance is displaced from that of the atomic resonance. As a result of that displacement, we have four poles in the expressions of Eqs. (11a) and (11b), which give rise to four peaks in the PES. If there was no electron-electron interaction, the atomic and core resonance energies would coincide and the four peaks of the PES would collapse to only two.

There is, however, a further more fundamental implication of that formal result. The two peaks obtained in that case do not reflect the transfer of the coherence established in the Rabi oscillation of one electron to the other, but simply the manifestation of the ac Stark splitting in the resonance transition of one electron to the PES of the same electron. That of course is to be expected since in that limit the electrons do not interact and therefore the PES consists of peaks originating from the ionization of noncommunicating electrons. It is the same as what is expected and has in fact been observed experimentally [17] in transitions where only one electron is active, as in the alkalies. It all seems naturally evident. What is not that evident is that the converse is also true; namely, that if a model produces only two symmetric peaks, it does not involve the transfer of the coherence from one strongly driven electron to the PES of the other, but simply the ac Stark splitting in the PES of one electron strongly driven between two of its own discrete states.

The above arguments might seem to not include the case in which the two-electron system does not have the equivalent of the atomic resonance, as is the case, for example, with H^-, which has only one bound (the ground) state $1s^2(^1S_0)$. In that case, however, the Rabi oscillation of one electron between $1s$ and $2p$ of the core (neutral H) while the other is in the continuum, is equivalent to the strong driving of the autodetaching resonance $2p\epsilon l$, which is the same as the Rabi oscillation of an autoionizing resonance having been discussed quite some time ago [6] and observed rather recently [7]. Care must then be taken in a theoretical modeling or experimental observation to distinguish it from the ac Stark splitting of the one-electron core (H) PES as it ionizes after detachment of one electron by single-photon absorption.

B. General pulse shape

In order to relate the theory to experiments, we must consider the effect of a realistic time-dependent pulse shape. We have shown in Ref. [19] that this is essential, since spectra depend critically on the intensity profile of the pulse. This is not surprising considering the time-dependent shifts and different paths to the continua. Each continuum state can be shifted through either of the four resonances (Fig. 2) several times during the pulse duration. A square pulse calculation has no chance of predicting the resulting interference (analogs to Ramsey interference) since it does not occur for a square pulse.

The square-pulse calculation is, however, quite helpful even when proceeding to a time-dependent calculation since the elimination of strongly coupled continua is carried out more conveniently in the energy domain (Appendix B). Equations (6d), (7a), and (7b) serve as a good starting point for a time-dependent calculation. It is straightforward to transform the equations back in the time domain, and to demonstrate the validity for time-dependent coupling strengths. Using Eqs. (8a)–(8d) we obtain the differential equations

$$i\frac{dC_g}{dt}=(E_g+I_{gg})C_g+(D_{g\bar{g}}+I_{g\bar{g}})C_{\bar{g}}, \tag{12a}$$

$$i\frac{dC_{\bar{g}}}{dt}=(E_{\bar{g}}+I_{\bar{g}\bar{g}})C_{\bar{g}}+(D_{\bar{g}g}+I_{\bar{g}g})C_g, \tag{12b}$$

$$i\frac{dC_c}{dt}=E_cC_c+D^{(2)}_{cg}C_g+D_{c\bar{g}}C_{\bar{g}}+D_{c\bar{c}}C_{\bar{c}}, \tag{12c}$$

$$i\frac{dC_{\bar{c}}}{dt}=E_{\bar{c}}C_{\bar{c}}+D^{(2)}_{\bar{c}g}C_{\bar{g}}+D_{\bar{c}c}C_c. \tag{12d}$$

This is just the Schrödinger equation providing the time evolution of the state vector $|\psi\rangle=C_g|g\rangle+C_{\bar{g}}|\bar{g}\rangle+\int dc(C_c|c\rangle+C_{\bar{c}}|\bar{c}\rangle)$ in the relevant subspace with the correct coupling parameters. The equations can be solved numerically thus providing the expansion coefficients and hence the PES $S(t,\epsilon_c)=|C_c|^2+|C_{\bar{c}}|^2$.

II. APPLICATION OF THE THEORY TO CALCIUM

The above calculation contains the minimum ingredients necessary for calculating a realistic PES obtained at near resonance. Besides the ionic and corresponding atomic transition, additional states might be important in specific cases. Near-resonant atomic states add to the number of interfering paths to the continua resulting in shifts, additional splittings, and/or different interference structure in the spectra. Excited ionic states are significant for the same as well as a few additional reasons. (a) They lead to photoelectron peaks corresponding to the respective ionic excited states. (b) The subsequent ionization of the populations left in these states leads to additional photoelectron peaks. Whether atomic and ionic states beside $|g\rangle$, $|\bar{g}\rangle$, $|c\rangle$, and $|\bar{c}\rangle$ need to be included in the calculation can only be determined from detailed knowledge of the atomic and ionic structure, as well as of the pulse.

The experiment on calcium by Walker *et al.* [1] was performed in a wavelength range from 380 to 405 nm (photon energy 24 700 to 26 300 cm^{-1}) using intensities ranging from 9 to 900 GW/cm^2. The ionic two-photon $4s$-$5s$ transition is within this frequency range (52 167 cm^{-1}), and it is therefore necessary to include the $5s$ state. The $6p$ state is located another 22 300 cm^{-1} higher in energy. The matrix elements involving this state are sufficiently small to ensure that it need not be included explicitly in the calculation, but

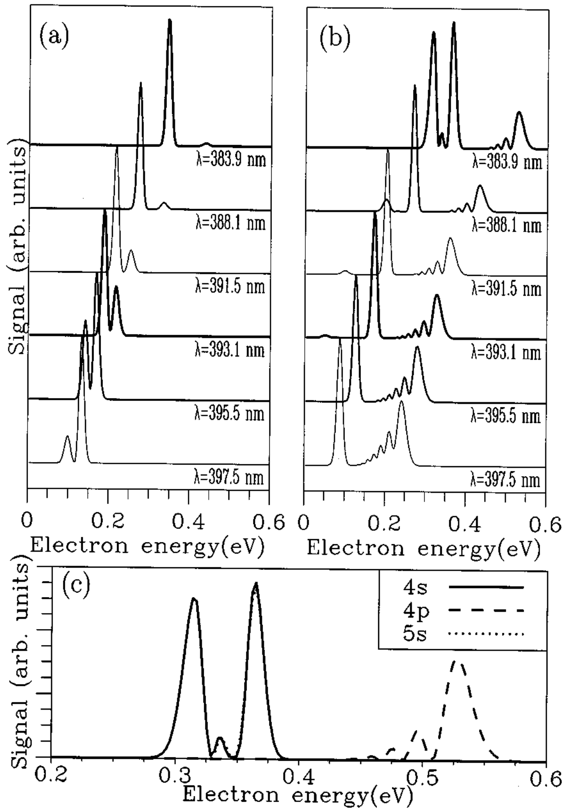

FIG. 3. Photoelectron energy spectra for several wavelengths at two intensities. The parameters chosen as cited in Fig. 2 of Ref. [1]. The pulse is Gaussian with full width duration $\tau=180$ fs at half maximum intensity (FWHM). (a) Peak intensity $I=10$ GW/cm^2. (b) $I=300$ GW/cm^2. For the high field spectrum there is very good agreement except for the longest wavelength giving peaks close to threshold, where our calculation is not expected to be precise. The low field should in principle be easier to calculate and yet the size of one peak seems to be overestimated by our calculation. The measured spectrum is, however, consistent with a somewhat lower peak intensity (approximately half) than the one given in [1]. Since intensity is very hard to measure precisely, this should not be of much concern. (c) The contributions from the various channels to the total spectrum at 383.9 nm in (b). The splittings reflect three-level system dynamics at the peak intensity.

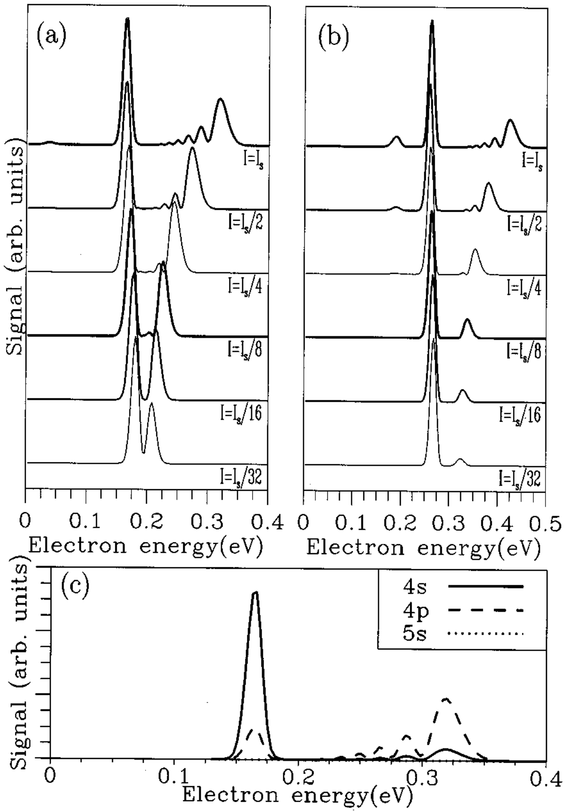

FIG. 4. Photoelectron energy spectra for several intensities on and off ionic resonance. The parameters are chosen as cited in Fig. 3 of Ref. [1]. The intensities are expressed in terms of the saturation intensity $I_s=300$ GW/cm. The pulse is Gaussian with $\tau=180$ fs (FWHM). (a) Wavelength $\lambda=393.5$ nm (on resonance), (b) $\lambda=388.5$ nm (off resonance). The agreement to experiment is excellent in both graphs taking into account the expected additional broadening due to spatial effects and possibly fine structure. (c) The contributions from the various channels to the total spectrum for $I=I_s$ on ionic resonance. The splitting occurs in both the $4s$ and $4p$ channel and is thus evidence of the continuum splitting in Fig. 2.

only through the linear Stark shift due to the multitude of nonresonant levels.

The modification of the above equations to include the effect of the ionic $5s$ state is straightforward both for the analytic result and for the differential equations. There seems to be little point in exhibiting the expressions. Instead we turn to results of calculations obtained for the range of laser parameters employed in the experiments of Walker *et al.* [1]. Our results are shown in Figs. 3, 4, and 5, which correspond to Figs. 2, 3, and 4 of Ref. [1]. Clearly all peaks observed in the experiment are also found in our *ab initio* calculated results. The relative heights are also the same in most cases. The analysis of the spectrum [Fig. 4(c)] reveals that the $4s$ and $4p$ continua contribute to both of the peaks of Fig. 2 (a). Thus, the spectra are indeed evidence of the electron correlation being manifested in a Rabi splitting.

A disagreement with the interpretation given in Ref. [1] is that its authors had not recognized the importance of ionization from the populations deposited during the pulse in the excited states $4p$ and $5s$. The most important implication of this is that a doublet of peaks around a photoelectron energy of 1.2 and 1.4 eV that could in principle be attributed to ac Stark splittings of the two-photon ionic transition $4s$-$5s$ or the one-photon $4p$-$5s$ turns out to be due to photoelectrons originating from these excited states. For the range of intensities cited in Ref. [1], the possibility of the above two ac Stark splittings can be safely ruled out. Any mixing of the ionic states should clearly show up as splittings in the individual channels [as in Fig. 4(c)]. Our Fig. 5(a) corresponding to the low energy part of the spectrum of Fig. 4 in Ref. [1], shows that this is not the case even for the highest intensities cited in Ref. [1].

On the other hand, population deposited in the ionic states during the pulse might subsequently be ionized. A four-, three-, or two-photon transition from the ionic $4s$, $4p$, or $5s$ states, respectively, will each give rise to a peak in the PES. Two peaks do indeed occur around 1.2 eV in the measured

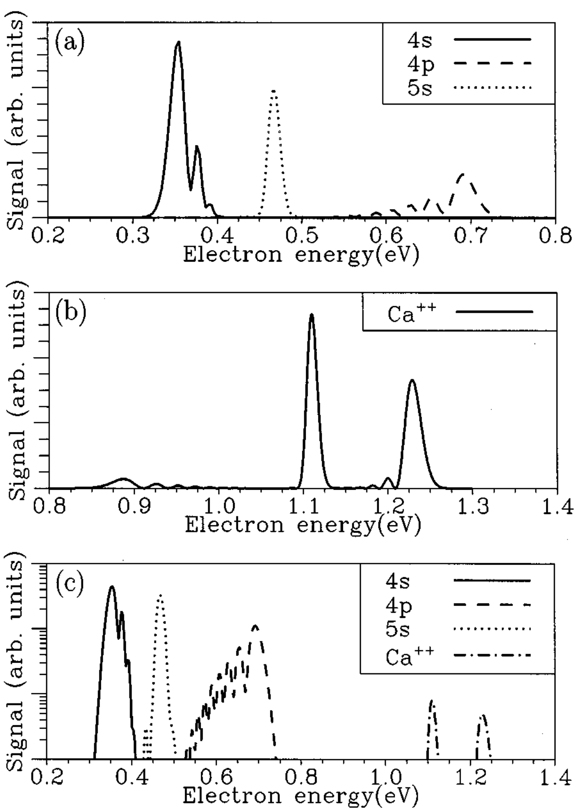

FIG. 5. Photoelectron energy spectra corresponding to (a) low and (b) intermediate photoelectron energy range of Fig. 4 in Ref. [1]. Note the linear scaling on the abscissa in the first two graphs. The wavelength is $\lambda = 381.3$ nm and the pulse Gaussian, duration $\tau = 180$ fs (FWHM). (a) Even at an intensity of $I = 800$ GW/cm^2, each peak can be attributed to a single continuum, showing that mixing is negligible. (b) A calculation treating the first and second ionization independently reproduces the features of the experimental data in the intermediate energy range. The three structures are due to ionization from the ionic states $4p$, $5s$, and $4s$, respectively. (c) The results of the two calculations are combined producing a spectrum very similar to the experimental. The peak due to ionization from the $4p$ state is too small to appear on this scale [the smallest peak in graph (b)].

PES [1], and we will now justify that they are due to ionization of ionic states.

It is relatively simple to test whether the calculated spectra in the low energy range of the spectrum are consistent with the observed double peak spectrum in the intermediate energy range. This can be done by calculating the population in each of the three ionic states after the pulse (by integration over the continua). The resulting numbers are taken as the initial conditions for a second and otherwise independent calculation of the response of a calcium ion to a similar pulse.

The result of such a calculation is shown in Fig. 5(b). Two relatively large peaks due to four-photon ionization of the large $4s$ population and two-photon ionization from the smaller $5s$ population are found. The nonresonant three-photon ionization of the $4p$ population gives rise to a considerably smaller peak. When the two spectra are put together, we obtain a spectrum (Fig. 5) very similar to the one presented in Fig. 4 of Ref. [1] for linearly polarized light. The use of circularly polarized light should make the $5s$ peaks disappear, as well as changing the Stark shifts. This is in full agreement with the experimental results.

We must emphasize that the single and double ionization processes are in principle not separable, even though this is what we have assumed in the above discussed calculation of the Ca^{2+} spectrum. The difference from a complete calculation is, however, expected to not be large in the present case, since the low energy part of the spectrum [Fig. 5(a)] shows that coherence is not important. The heights of all peaks of the doubly ionized species are expected to be somewhat overestimated by a common factor in the Ca^{2+} spectrum, while their positions should be more or less unaffected. The most serious remaining doubt about an independent calculation is probably that the ions are created mostly at peak intensity, rather than being present from the beginning of the pulse. In addition to influencing the peak heights as described, this could have other implications. After performing a calculation for a half Gaussian, however, we find that the picture does not change much, and therefore does not affect the conclusion: The two peaks observed are due to the subsequent ionization of the population deposited in ionic states by the first ionization step.

The question of the possible role of the fine structure of the core on the observed spectra needs to be addressed, as its importance has been debated in the literature [22,23]. The fine-structure splitting of the $4P_{3/2,1/2}$ doublet in Ca$^+$ is 226 cm^{-1}. Its chief influence on the physics of the process is that the core-resonant field drives not a two- but a three-level system which adds to the complexity of the overall behavior, without enriching the basic effects under investigation. On the contrary, it may be argued that the presence of fine-structure in the core is a nuisance, in the present context, detracting from the main line of the problem. But it is there nevertheless and the importance of its influence should be assessed.

The main concern of course here is whether it must be included in order to interpret the data published in Ref. [1]. A careful examination of the spectra in our Figs. 2, 3, and 4 provides the necessary clue. It is easy to verify by simple inspection that the photoelectron energy peaks having a $4p$ contribution are in general broader than the fine-structure splitting. In addition, our spectra having been obtained through equations that included only one $4p$ resonance are in very good agreement with the data published in Ref. [1]. It is thus reassuring that at least for the intensities employed in obtaining the data reported in Ref. [1], the fine structure is obscured by other effects that broaden the peaks. All such effects are included in our calculations which reproduce the data quite well.

The extension of our theory through the inclusion of one additional p state and the corresponding channels into the continuum presents no particular difficulty; it is in fact straightforward. We see, however, no reason to undertake such a task at this point as its value to the interpretation would be of secondary significance, and in connection to an effect of peripheral value to the issue at hand. This is rather fortunate, but not accidental as it enables the quantitative analysis to focus on the main issue. That it is not accidental, can be verified almost at the outset by simply estimating the main broadening mechanisms. Whether experimental data extending to intensities lower than those reported in Ref. [1] demand the inclusion of the fine structure of the core, as alluded to in Ref. [23], remains to be seen and may in fact be likely. For the time being, we shall leave our calculations where they stand as they provide the interpretation of data published thus far.

Finally, the exact position of the various peaks obtained in our calculation is somewhat displaced with respect to the experiment (typically by 10%). Since they are found to be quite sensitive to the intensity, one should not be too concerned about that. For a quantitative interpretation of all features of the data, we would need to know the uncertainty in the intensity (in each case) as well as the spatial features of the interaction volume. Furthermore, we checked whether our peak positions converge towards the zero field positions as they should. They do, while this does not seem to be true for the experimental data.

III. CONCLUSION

We have discussed the basic theory and have provided a comprehensive realistic formalism for the process of core-resonant ionization, with specific emphasis on the alkaline earth atoms. The main points of this theory are as follows. (a) The atomic core resonance is so close in energy to the core resonance transition that it must be included in the theoretical treatment, even if the field is in resonance with the core transition. (b) At the intensity required to produce observable Stark splitting, additional photon absorption in the atomic system will lead to significant production of excited ionic states. (c) These excited ionic states populated during the pulse ionize later on, producing further photoelectron peaks. (d) ac Stark shifts of magnitude varying in time during the pulse will produce additional structure in the PES.

A theoretical model and calculation aiming at predictions for the expected PES, or the interpretation thereof, must include at least all of the above processes and states, as well as a realistic description of the temporal shape of the pulse.

When put together in a complete calculation, these aspects produce a picture far more complex than a simple, symmetric doublet. And it is indeed such a complex picture that has emerged out of the recent experiments by Walker *et al.* [1]. We demonstrated very good agreement between the calculations and all published experimental data. Furthermore, the calculations were shown to give additional insight into the problem.

Last, we want to establish the close relation to another problem currently attracting much interest [11–13,24,25]. In the present paper, we have studied the effect of a strongly driven core resonance on an electron during ionization. More intricate effects are found when the electron leaving the core is slightly bound, so that it returns to the core in the form of a wave packet after a classical orbit time. The subsequent scatterings from the Rabi oscillating core has been shown to affect the shape of the wave packet strongly through electron-electron interaction and the resulting autoionization. The electron freed in this process leaves a Rabi oscillating core behind as in the scheme described here. A comprehensive study of that situation, which has been reported in brief [19], will be presented in a forthcoming paper.

APPENDIX A: THE CONTINUUM-CONTINUUM COUPLING STRENGTH

In this section, we show that $D_{c\overline{c}}$, which appeared in Eqs. (6), can be approximated as $\langle \mathrm{Ca}^+ 4s|d|\ \mathrm{Ca}^+ 4p\rangle$.

In general, the continuum wave function has an N-fold degeneracy corresponding to the N possible outgoing channels at a given energy [3,2,4]. Each channel A_i can be defined by antisymmetrized direct products of an ionic core state Φ and an angular momentum eigenstate χ of the outgoing (ionizing) electron. Denoting the radius of the outgoing electron by r, and the remaining coordinates by $\mathcal{R}$, the wave function c_i has the following asymptotic behavior for large r:

$$\langle \mathcal{R} r|c_i\rangle = \sum_j \ \langle \mathcal{R}|A_j\rangle \frac{1}{2r}[\delta_{ij}\phi^+_{j\epsilon'}(r) - S^\dagger_{ij}\phi^-_{j\epsilon'}(r)], \tag{A1}$$

where $\phi^{\pm}_{j\epsilon}(r) \simeq e^{\pm ikr+\delta_j}$, with δ_j the Coulomb phase shift determined by the angular momentum quantum number of the outgoing electron [5]. The S matrix represents the interaction between different channels due to the electron-electron Coulomb interaction.

Because of the indistinguishability of electrons, the dipole moment between two-electron wave functions consists of four terms: the inner-inner, the inner-outer, the outer-inner, and the outer-outer electron transitions. However, near the core-resonance frequency, the coupling strength between the two channels is dominated by the inner-inner electron transition, and can therefore be approximated as

$$\begin{aligned}\langle c_i|Q_c H\overline{Q_c}|\overline{c'_{i'}}\rangle \simeq &\sum_{jj'} \ \langle A_j|d|A_{j'}\rangle \frac{1}{4}\int \ dr[\delta_{ij}\phi^+_{j\epsilon}(r) \\ &-S^\dagger_{ij}\phi^-_{j\epsilon}(r)]^* \\ &\times[\delta_{i';j'}\phi^+_{j'\epsilon'}(r) - S'^\dagger_{i';j'}\phi^-_{j'\epsilon'}(r)] \\ \simeq &\sum_{jj'} \ \langle A_j|d|A_{j'}\rangle \Bigg[\delta(\epsilon-\epsilon') \\ &\times\frac{1}{2}(\delta_{ij}\delta_{i'j'} + S_{ij}S'^\dagger_{i'j'}) \\ &+ \frac{i}{2\pi\sqrt{k_j k_{j'}}}\left(\mathcal{P}\frac{\delta_{ij}\delta_{i'j'}}{k_{j'}-k_j} - \mathcal{P}\frac{S_{ij}S'^\dagger_{i'j'}}{k_{j'}-k_j}\right)\Bigg].\end{aligned} \tag{A2}$$

Now, we are ready to evaluate $\int dc' \langle\overline{c}|\overline{Q_c}HQ_c|c'\rangle G_{c'}$. Assuming that the coupling strengths $D^{(2)}_{cg}$ and $D^{(2)}_{c'g}$ (also $D_{c\overline{g}}$ and $D_{c'\overline{g}}$) are approximately equal, and so are $D_{c\overline{c}}$ and $D_{c'\overline{c}}$, then from Eq. (6c) we can derive $G_{c'} \simeq G_c(z-E_c/z-E_{c'})$. This leads to

$$\int dc'\langle\bar{c}|\bar{Q}_c H Q_c|c'\rangle G_{c'}\simeq\sum_{jj'}\langle A_j|d|A_{j'}\rangle \times\Bigg[\frac{1}{2}(\delta_{ij}\delta_{i'j'}+S_{ij}S'^{\dagger}_{i'j'}) +\frac{i}{2\pi}(\delta_{ij}\delta_{i'j'}-S_{ij}S'^{\dagger}_{i'j'}) \times\mathcal{P}\int dc'\frac{1}{\sqrt{k_jk_{j'}}(k_{j'}-k_j)} \times\frac{z-E_c}{z-E_{c'}}\Bigg]G_c, \tag{A3}$$

where $E_c=k_j^2/2$, $dc'=dE_{c'}=k_{j'}dk_{j'}$. The subscript labeling for c and c' has been omitted, having in mind that c corresponds to $A_i=4s\epsilon l$ and c' to $A_{i'}=4p\epsilon l$ channels.

The principal integral in the equation can be evaluated by the contour integral technique, and the result is simply $-i\pi$. Consequently, we obtain

$$\int dc'\langle\bar{c}|\bar{Q}_c H Q_c|c'\rangle G_{c'}\simeq\langle A_i|d|A_{i'}\rangle G_c. \tag{A4}$$

By definition, we have $D_{cc'}=\langle A_i|d|A_{i'}\rangle=\langle\Phi_i|d|\Phi'_i\rangle\langle\chi|\chi\rangle=\langle\Phi_i|d|\Phi'_i\rangle\delta_{\chi,\chi'}$. For the specific system we consider in the paper, we have $D_{c\langle c|}=\langle \mathrm{Ca}^+4s|d|\,\mathrm{Ca}^+4p\rangle$, for $|\chi'\rangle=|\chi\rangle=|s\rangle$ or $|d\rangle$. Note that this conclusion is valid as long as the assumption that $(z-E_c)G_c$ varies slowly holds. It is remarkable that complicated channel couplings represented by S matrices of the continua do not manifest themselves in the core resonance coupling of the two continua.

APPENDIX B: ELIMINATION OF STRONGLY COUPLED CONTINUA

The elimination of continua is a widely used method of determining the influence of a ''bath'' with infinite degrees of freedom on a system with just a few. In the present case the ''bath'' is the electron continuum. It seems, however, that the elimination of strongly coupled continua has not been discussed in the literature until now. This is despite the fact that it does *not*, in general, lead to ordinary shifts and widths, which has apparently been taken for granted when the strong coupling of continua was not simply neglected.

Though we treat only a special case of this elimination, the methods are applicable in general. Comparing the equations (5a) and (5b) with (7a) and (7b), we have

$$I_{gg}(z)G_g+I_{g\bar{g}}(z)G_{\bar{g}}=\int dcD^{(2)}_{gc}G_c \tag{B1a}$$

$$I_{\bar{g}\bar{g}}(z)G_{\bar{g}}+I_{\bar{g}g}(z)G_g=\int dc(D^{(2)}_{\bar{g}\bar{c}}G_{\bar{c}}+D_{\bar{g}c}G_c). \tag{B1b}$$

Using the expressions (7c) and (7d) for G_c and $G_{\bar{c}}$ we obtain explicit expressions for the shift-width integrals in terms of integrals over coupled states ($|c\rangle$, $|\bar{c}\rangle$).

$$I_{gg}(z)=\int dc\frac{D^{(2)}_{gc}(z-E_{\bar{c}})D^{(2)}_{cg}}{(z-E_c)(z-E_{\bar{c}})-|D_{c\bar{c}}|^2}, \tag{B2a}$$

$$I_{g\bar{g}}(z)=\int dc\frac{D^{(2)}_{gc}(z-E_{\bar{c}})D_{c\bar{g}}+D^{(2)}_{gc}D_{c\bar{c}}D^{(2)}_{\bar{c}\bar{g}}}{(z-E_c)(z-E_{\bar{c}})-|D_{c\bar{c}}|^2}, \tag{B2b}$$

$$I_{\bar{g}g}(z)=\int dc\frac{D^{(2)}_{\bar{g}\bar{c}}D_{\bar{c}c}D^{(2)}_{cg}+D_{\bar{g}c}(z-E_{\bar{c}})D^{(2)}_{cg}}{(z-E_c)(z-E_{\bar{c}})-|D_{c\bar{c}}|^2}, \tag{B2c}$$

$$I_{\bar{g}\bar{g}}(z)=\int dc\frac{D_{\bar{g}c}(z-E_{\bar{c}})D_{c\bar{g}}+D_{\bar{g}c}D_{c\bar{c}}D^{(2)}_{\bar{c}\bar{g}}+D^{(2)}_{\bar{g}\bar{c}}D_{\bar{c}c}D_{c\bar{g}}+D^{(2)}_{\bar{g}\bar{c}}(z-E_c)D^{(2)}_{\bar{c}\bar{g}}}{(z-E_c)(z-E_{\bar{c}})-|D_{c\bar{c}}|^2}. \tag{B2d}$$

These integrals are obviously different from the normal integrals over continuum states encountered when continua are eliminated [20], and only under certain conditions do they reduce to the normal shifts and widths. It is useful to define the z-dependent solutions $E_c^{\pm}$ of the equation

$$(E_c^+-E_c)(E_c^--E_c)\equiv(z-E_c)(z-E_c+\Delta_c)-|D_{c\bar{c}}|^2. \tag{B3}$$

Please note the similarity and difference to Eq. (9b) defining the quantities $z_c^{\pm}$. Unlike those, $E_c^{\pm}$ does not depend on the pair of continuum states ($|c\rangle$, $|\bar{c}\rangle$) since the coupling strength $D_{c\bar{c}}$ does not. The fractions are now expanded yielding rather lengthy expressions. For convenience we define normal shift-width integrals

$$W_{gg}(E)\equiv\int dc\frac{|D^{(2)}_{cg}|^2}{E-E_c},\quad W_{\bar{g}g}(E)\equiv\int dc\frac{D_{\bar{g}c}D^{(2)}_{cg}}{E-E_c},$$

$$W_{g\bar{g}}(E)\equiv\int dc\frac{D^{(2)}_{gc}D_{c\bar{g}}}{E-E_c},\quad W^{c}_{\bar{g}\bar{g}}(E)\equiv\int dc\frac{D_{\bar{g}c}D_{c\bar{g}}}{E-E_c},$$

$$W^{\bar c}_{\bar g g}(E)\equiv\int dc\,\frac{D^{(2)}_{\bar g\bar c}D^{(2)}_{\bar c g}}{E-E_c},$$

and matrix elements

$$T^{c\bar c}_{\bar g g}(E)\equiv\int dc\frac{D_{\bar g c}D_{c\bar c}D^{(2)}_{\bar c g}}{E-E_c},$$

$$T^{\bar c\bar c}_{\bar g g}(E)\equiv\int dc\,\frac{D^{(2)}_{\bar g\bar c}D_{\bar c\bar c}D_{\bar c g}}{E-E_c},$$

$$T^{c\bar c}_{g\bar g}(E)\equiv\int dc\,\frac{D^{(2)}_{gc}D_{c\bar c}D^{(2)}_{\bar c\bar g}}{E-E_c},$$

$$T^{\bar c\bar c}_{\bar g\bar g}(E)\equiv\int dc\,\frac{D^{(2)}_{\bar g\bar c}D_{\bar c\bar c}D^{(2)}_{cg}}{E-E_c}.$$

Expressed in terms of these quantities, Eqs. (B2a)–(B2d) become

$$I_{gg}(z)=\frac{-1}{E_c^+-E_c^-}[(z-E_c^++\Delta_c)W_{gg}(E_c^+)$$
$$-(z-E_c^-+\Delta_c)W_{gg}(E_c^-)], \tag{B4a}$$

$$I_{g\bar g}(z)=\frac{-1}{E_c^+-E_c^-}[(z-E_c^++\Delta_c)W_{g\bar g}(E_c^+)$$
$$-(z-E_c^-+\Delta_c)W_{g\bar g}(E_c^-)$$
$$+T^{c\bar c}_{g\bar g}(E_c^+)-T^{c\bar c}_{g\bar g}(E_c^-)], \tag{B4b}$$

$$I_{\bar g\bar g}(z)=\frac{-1}{E_c^+-E_c^-}[(z-E_c^++\Delta_c)W_{\bar g\bar g}(E_c^+)$$
$$-(z-E_c^-+\Delta_c)W_{\bar g\bar g}(E_c^-)$$
$$+T^{\bar c\bar c}_{\bar g\bar g}(E_c^+)-T^{\bar c\bar c}_{\bar g\bar g}(E_c^-)], \tag{B4c}$$

$$I_{\bar g g}(z)=\frac{-1}{E_c^+-E_c^-}[(z-E_c^+)W^{\bar c}_{\bar g g}(E_c^+)-(z-E_c^-)W^{\bar c}_{\bar g g}(E_c^-)$$
$$+T^{\bar c\bar c}_{\bar g g}(E_c^+)-T^{\bar c\bar c}_{\bar g g}(E_c^-)+(z-E_c^++\Delta_c)W^{c}_{\bar g g}(E_c^+)$$
$$-(z-E_c^-+\Delta_c)W^{c}_{\bar g g}(E_c^-)+T^{c\bar c}_{\bar g g}(E_c^+)-T^{c\bar c}_{\bar g g}(E_c^-)]. \tag{B4d}$$

From the definition (B3) of $E_c^{\pm}$ we have

$$E_c^{\pm}=z+\Delta_c/2\pm\tilde\Omega_c/2\equiv E_c^0\pm\tilde\Omega_c/2 \tag{B5}$$

and therefore

$$I_{gg}(z)=\frac{-1}{2\tilde\Omega_c}[(\Delta_c-\tilde\Omega_c)W_{gg}(E_c^+)-(\Delta_c+\tilde\Omega_c)W_{gg}(E_c^-)], \tag{B6a}$$

$$I_{g\bar g}(z)=\frac{-1}{2\tilde\Omega_c}\{(\Delta_c-\tilde\Omega_c)W_{g\bar g}(E_c^+)-(\Delta_c+\tilde\Omega_c)W_{g\bar g}(E_c^-)$$
$$+2[\mathrm{T}^{c\bar c}_{g\bar g}(\mathrm{E}_c^+)-\mathrm{T}^{c\bar c}_{g\bar g}(\mathrm{E}_c^-)]\}, \tag{B6b}$$

$$I_{\bar g\bar g}(z)=\frac{-1}{2\tilde\Omega_c}\{(\Delta_c-\tilde\Omega_c)W_{\bar g\bar g}(E_c^+)-(\Delta_c+\tilde\Omega_c)W_{\bar g\bar g}(E_c^-)$$
$$+2[T^{\bar c\bar c}_{\bar g\bar g}(E_c^+)-T^{\bar c\bar c}_{\bar g\bar g}(E_c^-)]\}, \tag{B6c}$$

$$I_{\bar g g}(z)=\frac{-1}{2\tilde\Omega_c}\{(\Delta_c-\tilde\Omega_c)W^{c}_{\bar g g}(E_c^+)-(\Delta_c+\tilde\Omega_c)W^{c}_{\bar g g}(E_c^-)$$
$$+2[T^{c\bar c}_{\bar g g}(E_c^+)-T^{c\bar c}_{\bar g g}(E_c^-)]+(-\Delta_c-\tilde\Omega_c)W^{\bar c}_{\bar g g}(E_c^+)$$
$$-(-\Delta_c+\tilde\Omega_c)W^{\bar c}_{\bar g g}(E_c^-)$$
$$+2[T^{\bar c\bar c}_{\bar g g}(E_c^+)-T^{\bar c\bar c}_{\bar g g}(E_c^-)]\}. \tag{B6d}$$

Equations (B4a)–(B4d) now reduce to

$$I_{gg}(z)=\frac{-\Delta_c[W_{gg}(E_c^+)-W_{gg}(E_c^-)]}{2\tilde\Omega_c}$$
$$+\frac{W_{gg}(E_c^+)+W_{gg}(E_c^-)}{2}, \tag{B7a}$$

$$I_{g\bar g}(z)=\frac{-\Delta_c[W_{g\bar g}(E_c^+)-W_{g\bar g}(E_c^-)]}{2\tilde\Omega_c}$$
$$+\frac{W_{g\bar g}(E_c^+)+W_{g\bar g}(E_c^-)}{2}-\frac{T^{c\bar c}_{g\bar g}(E_c^+)-T^{c\bar c}_{g\bar g}(E_c^-)}{\tilde\Omega_c}, \tag{B7b}$$

$$I_{\bar g\bar g}(z)=\frac{-\Delta_c[W_{\bar g\bar g}(E_c^+)-W_{\bar g\bar g}(E_c^-)]}{2\tilde\Omega_c}$$
$$+\frac{W_{\bar g\bar g}(E_c^+)+W_{\bar g\bar g}(E_c^-)}{2}-\frac{T^{\bar c\bar c}_{\bar g\bar g}(E_c^+)-T^{\bar c\bar c}_{\bar g\bar g}(E_c^-)}{\tilde\Omega_c}, \tag{B7c}$$

$$I_{\bar g g}(z)$$
$$=\frac{-\Delta_c[W^{c}_{\bar g g}(E_c^+)-W^{c}_{\bar g g}(E_c^-)-W^{\bar c}_{\bar g g}(E_c^+)+W^{\bar c}_{\bar g g}(E_c^-)]}{2\tilde\Omega_c}$$
$$+\frac{W^{c}_{\bar g g}(E_c^+)+W^{c}_{\bar g g}(E_c^-)+W^{\bar c}_{\bar g g}(E_c^+)+W^{\bar c}_{\bar g g}(E_c^-)}{2}$$
$$-\frac{T^{c\bar c}_{\bar g g}(E_c^+)-T^{c\bar c}_{\bar g g}(E_c^-)+T^{\bar c\bar c}_{\bar g g}(E_c^+)-T^{\bar c\bar c}_{\bar g g}(E_c^-)}{\tilde\Omega_c}. \tag{B7d}$$

We have gone this far without making any approximations. The normal pole approximation can now be carried out yielding shifts and widths for each of the integrals provided the continua are smooth around the energy of each of the dressed bound states plus and minus half an ionic Rabi frequency. This happens if the continua are without structure and if the energies are not too close to threshold. The resulting expressions, nevertheless, do not reduce to the normal shifts and widths unless certain conditions are fulfilled. The expressions reduce significantly if the shifts and widths vary approximately linearly over an energy range given by the Rabi frequency

$$I_{gg}(z)=W_{gg}(E_0)-\frac{\Delta_c}{2}\left.\frac{dW_{gg}}{dE}\right|_{E=E_0}, \tag{B8a}$$

$$I_{g\bar{g}}(z)=W_{g\bar{g}}(E_0)-\frac{\Delta_c}{2}\left.\frac{dW_{g\bar{g}}}{dE}\right|_{E=E_0}-\left.\frac{dT^{c\bar{c}}_{g\bar{g}}}{dE}\right|_{E=E_0}, \tag{B8b}$$

$$I_{\bar{g}g}(z)=W_{\bar{g}g}(E_0)-\frac{\Delta_c}{2}\left.\frac{dW_{\bar{g}g}}{dE}\right|_{E=E_0}-\left.\frac{dT^{\bar{c}c}_{\bar{g}g}}{dE}\right|_{E=E_0}, \tag{B8c}$$

$$I_{\bar{g}\bar{g}}(z)=W^{\bar{c}}_{g\bar{g}}(E_0)+W^{c}_{\bar{g}g}(E_0)-\frac{\Delta_c}{2}\left(\frac{dW^{c}_{\bar{g}g}}{dE}-\frac{dW^{\bar{c}}_{g\bar{g}}}{dE}\right)_{E=E_0}-\left(\frac{dT^{c\bar{c}}_{\bar{g}\bar{g}}}{dE}-\frac{dT^{\bar{c}c}_{\bar{g}\bar{g}}}{dE}\right)_{E=E_0}. \tag{B8d}$$

Note that even though $E_c^0=z+\Delta_c/2$, the derivatives are intensity independent in the linear approximation, except for the trivial intensity dependence of the matrix elements. We can go one step further, if the coupling strengths can be considered constant over a range given by the Rabi frequency. In this case the derivatives vanish, and we are left with the normal shifts and widths, i.e., those that would be expected if the core coupling was neglected completely in the calculation of the shifts [strictly speaking, the coupling strengths need only be equal at the four peak positions (square pulse), which in practice means constant over the whole range]. This is exactly the assumption we have made in order to obtain the simple expressions (8a) and (8b). We therefore do not expect to have good results if one or more peaks during the pulse gets close to threshold. Note, however, that we could go beyond this approximation — we only need to calculate more coupling strengths.

APPENDIX C: LIMITATIONS ON THE VALIDITY OF THE TREATMENT

Equations (7c) and (7d) were derived under the assumption that the coupling of continua is purely discrete due to the discrete core transition. This requirement cannot be fulfilled unless the ignored integrals

$$\int dc' B_{c'\bar{c}}G_{\bar{c}}\equiv J_{c'g}G_g+J_{c'\bar{g}}G_{\bar{g}}, \tag{C1}$$

$$\int dc B_{\bar{c}'c}G_c\equiv J_{\bar{c}'g}G_g+J_{\bar{c}'\bar{g}}G_{\bar{g}}, \tag{C2}$$

are themselves small compared to other couplings in this approximation, with above equations serving as definitions of $B_{c'\bar{c}}$ and $B_{\bar{c}'c}$.

By direct analogy to calculations done in Appendix B, we obtain in the linear approximation

$$J_{c'g}(z)=-\left.\frac{dS_{c'g}}{dE}\right|_{E=E_0}, \tag{C3a}$$

$$J_{c'\bar{g}}(z)=V_{c'\bar{g}}(E_0)+\frac{\Delta_c}{2}\left.\frac{dV_{c'\bar{g}}}{dE}\right|_{E=E_0}-\left.\frac{dS_{c'\bar{g}}}{dE}\right|_{E=E_0}, \tag{C3b}$$

$$J_{\bar{c}'g}(z)=V_{\bar{c}'g}(E_0)-\frac{\Delta_c}{2}\left.\frac{dV_{\bar{c}'g}}{dE}\right|_{E=E_0}, \tag{C3c}$$

$$J_{\bar{c}'\bar{g}}(z)=V_{\bar{c}'\bar{g}}(E_0)+-\ \frac{\Delta_c}{2}\left.\frac{dV_{\bar{c}'\bar{g}}}{dE}\right|_{E=E_0}-\left.\frac{S_{\bar{c}'\bar{g}}}{dE}\right|_{E=E_0}. \tag{C3d}$$

where

$$V_{c'\bar{g}}(E)\equiv\int dc\frac{B_{c'\bar{c}}D^{(2)}_{\bar{c}g}}{E-E_c},\quad S_{c'g}(E)\equiv\int dc\frac{B_{c'\bar{c}}D_{\bar{c}c}D^{(2)}_{cg}}{E-E_c},$$

$$V_{\bar{c}'g}(E)\equiv\int dc\frac{B_{\bar{c}'c}D^{(2)}_{cg}}{E-E_c},\quad S_{c'\bar{g}}(E)\equiv\int dc\frac{B_{c'\bar{c}}D_{\bar{c}c}D_{c\bar{g}}}{E-E_c},$$

$$V_{\bar{c}'\bar{g}}(E)\equiv\int dc\frac{B_{\bar{c}'c}D_{c\bar{g}}}{E-E_c},\quad S_{\bar{c}'g}(E)\equiv\int dc\frac{B_{\bar{c}'c}D_{c\bar{c}}D^{(2)}_{\bar{c}g}}{E-E_c}.$$

Assuming constant coupling strengths over an energy range given by the core transition Rabi frequency (see Appendix B) makes the derivatives in Eqs. (C3a)–(C3d) vanish. The resulting couplings, which were neglected in our treatment, must be small compared to the couplings which were included, i.e.,

$$|J_{c\bar{g}}|\simeq|V_{c\bar{g}}|\ll|D_{c\bar{g}}|, \tag{C4a}$$

$$|J_{\bar{c}g}|\simeq|V_{\bar{c}g}|\simeq 0, \tag{C4b}$$

$$|J_{\bar{c}\bar{g}}|\simeq|V_{\bar{c}\bar{g}}|\ll|D^{(2)}_{\bar{c}g}|. \tag{C4c}$$

The second of these conditions reflects that no other coupling between states $|g\rangle$ and $|\bar{c}\rangle$ are present in Eq. (5d). This coupling therefore needs to be negligible compared to other couplings to $|\bar{c}\rangle$.

Finally, we must consider when these conditions for a reliable treatment are fulfilled. The matrix elements of B are proportional to the core transition matrix element and thus to the field amplitude. The left-hand side of the first condition (C4a) is therefore third order in field amplitude while the right-hand side is second order. Similarly, the left-hand side of the second condition is third order in intensity while the other couplings to $|\bar{c}\rangle$ are of lower order. Both requirements are therefore expected to be fulfilled if the intensity is not too high, which means here such that the Rabi frequency is smaller than the energy difference of the $4p$ from the $5p$. For Ca this implies less than 10^{13} W/cm^2.

Both sides are second order in field amplitude in the last condition (C4c). Both couplings must therefore be small compared to other couplings to the state $|\overline{c}\rangle$. This amounts to requiring that the continuum $|\overline{c}\rangle$ is mainly populated through Rabi oscillation in the core or two-photon transitions from $|\overline{g}\rangle$ involving the $|c\rangle$ continuum and the discrete part of the $|c\rangle$-$|\overline{c}\rangle$ coupling. This is certainly the case, and we can conclude that the treatment is expected to be valid in the present case. The validity can in any case be checked directly by calculating the integrals involved.

[1] B. Walker *et al.*, Phys. Rev. Lett. **75**, 633 (1995).
[2] K. T. Lu, Phys. Rev. A **4**, 579 (1971).
[3] M. J. Seaton, Rep. Prog. Phys. **46**, 167 (1983).
[4] C. H. Greene and L. Kim, Phys. Rev. A **36**, 2706 (1987).
[5] H. Friedrich, *Theoretical Atomic Physics* (Springer-Verlag, Berlin, 1991).
[6] P. Lambropoulos and P. Zoller, Phys. Rev. A **24**, 379 (1981).
[7] N. E. Karapanagioti, O. Faucher, Y. L. Shao, and D. Charalambidis, Phys. Rev. Lett. **74**, 2431 (1995).
[8] S. J. van Enk, Jian Zhang, and P. Lambropoulos, Appl. Phys. B **60**, S141 (1995).
[9] T. F. Gallagher, *Rydberg Atoms* (Cambridge University Press, England, 1994).
[10] U. Eichmann, V. Lange, and W. Sandner, Phys. Rev. Lett. **64**, 274 (1990).
[11] L. G. Hanson and P. Lambropoulos, Phys. Rev. Lett. **74**, 5009 (1995).
[12] O. Zobay and G. Alber, Phys. Rev. A **52**, 541 (1995).
[13] F. Robicheaux, Phys. Rev. A **47**, 1391 (1993).
[14] R. Grobe and J. H. Eberly, Phys. Rev. A **48**, 623 (1993).
[15] B. R. Mollow, Phys. Rev. **188**, 1969 (1969).
[16] A. T. Georges and P. Lambropoulos, Phys. Rev. A **18**, 587 (1978).
[17] W. Nicklich *et al.*, Phys. Rev. Lett. **69**, 3455 (1992).
[18] R. Grobe and S. L. Haan, J. Phys. B **27**, L735 (1994).
[19] L. G. Hanson, Jian Zhang, and P. Lambropoulos, Europhys. Lett. **30**, 81 (1995); see also S. L. Haan and R. Grobe, *ibid.* **33**, 247 (1996); L. G. Hanson, Jian Zhang, and P. Lambropoulos, *ibid.* **33**, 251 (1996).
[20] C. Cohen-Tannoudji, J. Dupont-Roc, and G. Grynberg, *Atom-Photon Interactions* (John Wiley and Sons, New York, 1992).
[21] P. Lambropoulos, *Advances in Atomic and Molecular Physics* (Academic Press, New York, 1976), p. 87.
[22] L. G. Hanson, Jian Zhang, and P. Lambropoulos, Phys. Rev. Lett. **77**, 202 (1996).
[23] B. Walker *et al.*, Phys. Rev. Lett. **77**, 203 (1996).
[24] N. J. van Druten and H. G. Muller, Phys. Rev. A **52**, 3047 (1995).
[25] N. J. van Druten and H. G. Muller, J. Phys. B **29**, 15 (1996).